J. Iron Steel Res. Int. (2023) 30:1916–1920
https://doi.org/10.1007/s42243-022-00893-2

SHORT COMMUNICATION

Chemical patterning enhanced by increasing quenching temperature in a medium-Mn steel

Chao Zhang[1] · Zhi-ping Xiong[1,2] · De-zhen Yang[1] · Valeriy Dudko[3] · Xing-wang Cheng[1,2]

Received: 10 August 2022 / Revised: 27 September 2022 / Accepted: 25 November 2022 / Published online: 14 February 2023

Abstract
Chemical heterogeneity in high-temperature austenite is an effective way to tune the austenite-to-martensite transformation during cooling. The effect of quenching temperature on microstructure evolution is investigated when the high-temperature austenite is heterogeneous. After fast austenitization from partitioned pearlite consisting of Mn-enriched cementite and Mn-depleted ferrite in Fe–0.29C–3.76Mn–1.50Si (wt.%) steel, quenching to room temperature and quenching to 130 °C followed by 400 °C partitioning are both applied. With increasing quenching temperature from 25 to 130 °C, the amount of heterogeneous microstructure (lamellar ghost pearlite) increases from 10.6% to 33.6% and the thickness of Mn-enriched retained austenite film is increased from 31.9 ± 5.9 to 51.5 ± 4.4 nm, indicating an enhancement of chemical patterning. It is probably ascribed to the reduction in driving force for austenite-to-martensite transformation, which requires a lower Mn content for austenite retention.

Keywords Heterogeneous microstructure · Phase transformation · Retained austenite · Quenching temperature · Chemical patterning

1 Introduction

Advanced high-strength steels with excellent combination of strength and ductility are under continuous development in order to satisfy the increasing requirement of safety and weight reduction [1–5]. Recently, chemical heterogeneity has been demonstrated as an efficient strategy for microstructure modification and mechanical properties enhancement in medium-Mn steels [6, 7]. The chemical heterogeneity in high-temperature austenite can strongly alter the austenite-to-martensite transformation during quenching process. The microstructures consisting of Mn-depleted ferrite and Mn-enriched retained austenite (RA) were produced by intercritical annealing in an Fe–0.18C–8.0Mn (wt.%) steel. After fast austenitization, the high-temperature austenite inherited the Mn heterogeneous distribution, leading to the formation of so-called chemical boundaries. During quenching to room temperature, fine martensitic laths and RA were obtained due to the obstructive effect of chemical boundaries on austenite-to-martensite transformation [7]. Similarly, Sun et al. [6] produced alternative film RA and martensitic lath (ghost pearlite, GP) through fast austenitization from lamellar pearlite consisting of Mn-enriched cementite and Mn-depleted ferrite in an Fe–0.51C–4.35Mn (wt.%) steel, which is so-called chemical patterning.

Until now, many published literatures try to retain chemical heterogeneity in high-temperature austenite through fast heating and short austenitization [8–12]. A lower austenitization temperature and a shorter holding time can help retain the chemical heterogeneity present in the initial microstructure. Additionally, the samples were all quenched to room temperature and as a result, the final microstructure was chemically patterned [6, 7]. It is well-known that quenching temperature can affect austenite-to-martensite transformation by changing its driving force [13–17]. In the present study, quenching temperature is

✉ Zhi-ping Xiong
zpxiong@bit.edu.cn; zuileniwota@126.com

[1] National Key Laboratory of Science and Technology on Materials under Shock and Impact, Beijing Institute of Technology, Beijing 100081, China

[2] Tangshan Research Institute, Beijing Institute of Technology, Tangshan 063000, Hebei, China

[3] Belgorod State University, Belgorod 308015, Russia

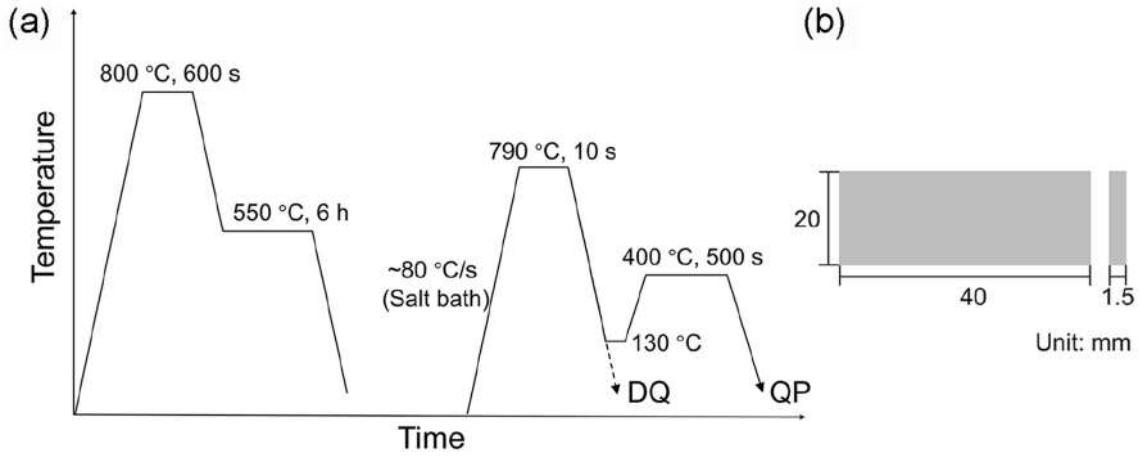

Fig. 1 Illustration of heat treatment (**a**) and sample dimension (**b**)

proposed to tune the austenite-to-martensite transformation from heterogeneous high-temperature austenite, indicating that a higher quenching temperature can enhance the chemical patterning and, namely, increase the GP fraction and the width of film RA in GP. This study provides a feasible way to tune the chemical patterning simply through the adjustment of quenching temperature.

2 Experimental

The chemical composition of hot-rolled steel is Fe–0.29C–3.76Mn–1.50Si (wt.%). The heat treatment is schematically illustrated in Fig. 1a. The samples were firstly austenized at 800 °C for 600 s in a muffle furnace, then transferred to a salt bath furnace (550 °C) and held for 6 h in order to obtain full pearlite. Subsequently, the samples were machined into 40 mm × 20 mm × 1.5 mm (Fig. 1b). Following this, they were fast heated to 790 °C at a rate of ~ 80 °C/s and held for 10 s in a salt bath. Finally, the samples were quenched to room temperature (DQ) or quenched into an oil bath of 130 °C and quickly moved to another salt bath (400 °C) for 500 s (QP). The microstructures were characterized using a scanning electron microscope (SEM) and a transmission electron microscope (TEM) equipped with an energy-dispersive spectroscope (EDS) and X-ray diffraction (XRD). The Mn content was described by the *U*-fraction (U_{Mn}) that indicates the substitutional sites occupied by Mn atoms [6, 18]. In the present study, the U_{Mn} was calculated by $x_{Mn}/(x_{Mn} + x_{Fe} + x_{Si})$ where x_{Mn}, x_{Fe} and x_{Si} represent their atomic fractions.

3 Results and discussion

Figure 2 shows the partitioned pearlite after 6 h holding at 550 °C, which consists of ferrite and cementite. Lamellar and spherical pearlites are both observed, among which the fraction of lamellar pearlite is 65.3% ± 2.2%. Strong Mn heterogeneity is detected by TEM-EDS (Fig. 2b). As an example of lamellar pearlite, Mn is enriched in cementite with U_{Mn} of 17.6% ± 1.2% while Mn is depleted in ferrite fluctuating around U_{Mn} = 1.4%–1.8%. The thickness of

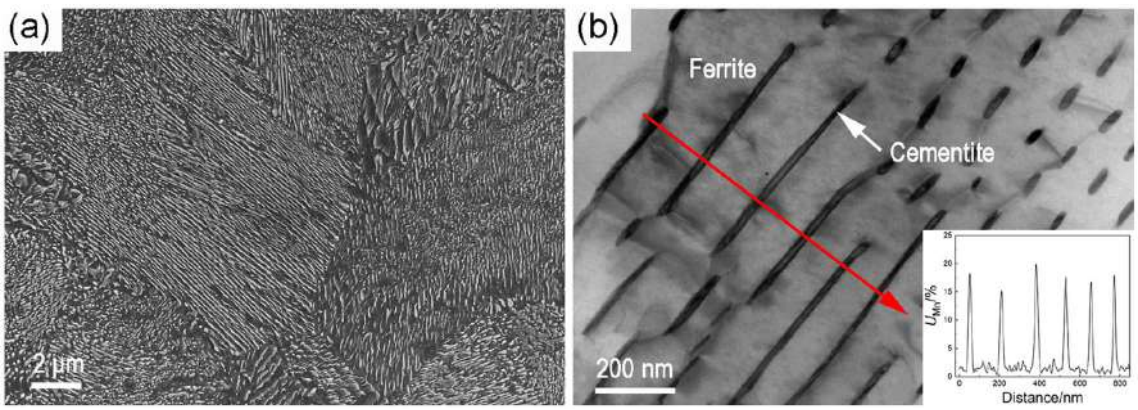

Fig. 2 SEM image (**a**) and TEM bright-field image (**b**) of partitioned pearlite after holding at 550 °C for 6 h

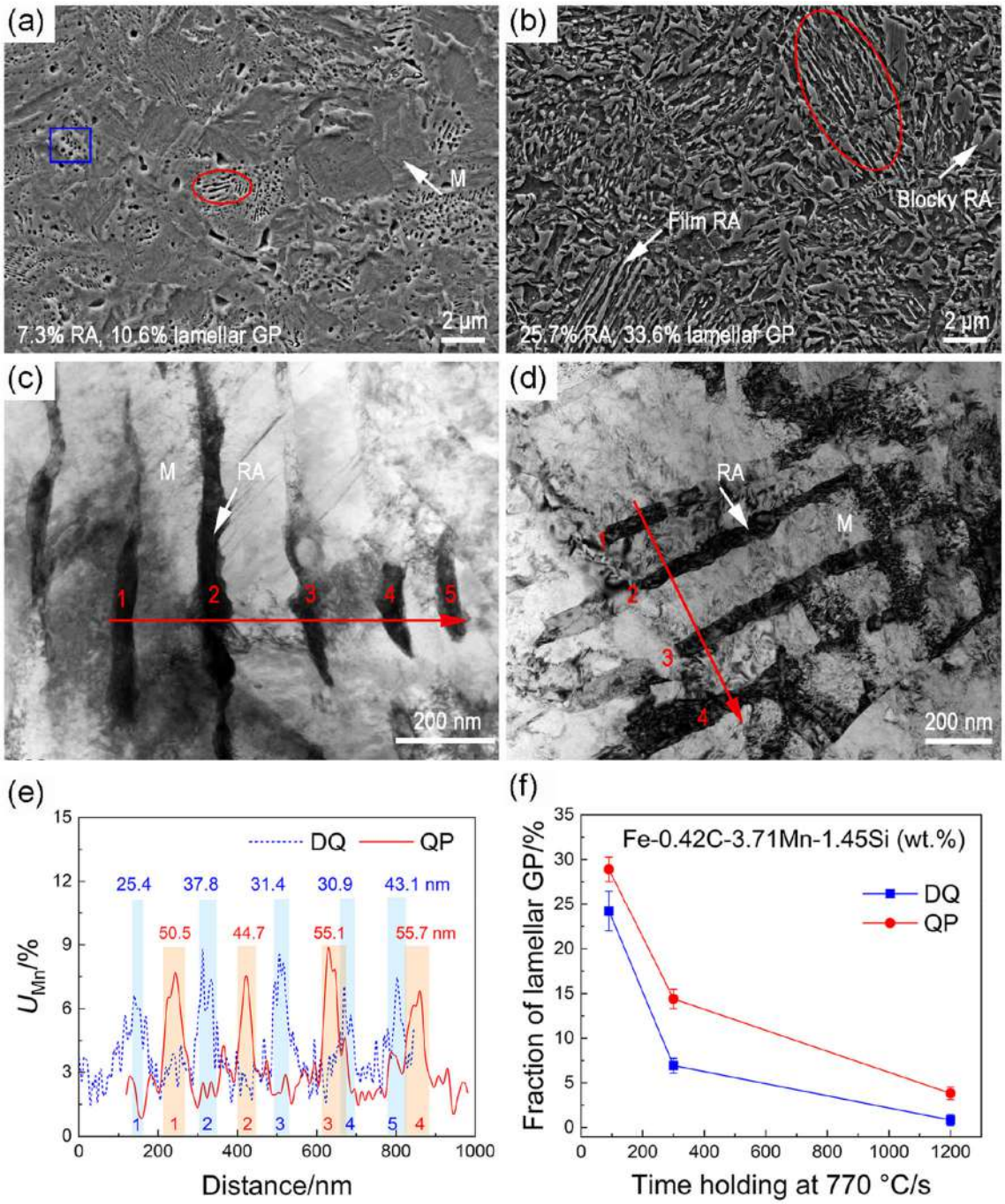

Fig. 3 SEM images (**a**, **b**) and TEM bright-field images (**c**, **d**) of DQ (**a**, **c**) and QP (**b**, **d**) samples, TEM-EDS line scanning corresponding to lines in **c**, **d** (**e**), and evolution of lamellar GP fraction in DQ and QP Fe–0.42C–3.71Mn–1.45Si steel (**f**)

lamellar cementite and ferrite is 14.6 ± 3.6 and 129.2 ± 22.5 nm, respectively.

Figure 3a, b shows the microstructures after quenching at different temperatures following austenitization at 790 °C for 10 s. In DQ sample, both lamellar (red circle) and spherical (blue rectangle) GP, which exhibit similar microstructures to the lamellar and spherical pearlite, are observed. It indicates the inheritance of Mn heterogeneity and, in turn, chemical patterning, as demonstrated in Refs. [6, 19, 20]. Whereas, in QP sample, the lamellar GP is clearly seen while the spherical GP cannot be clearly distinguished due to carbides precipitation during partitioning stage.

Increasing quenching temperature from 25 to 130 °C significantly increases the fraction of lamellar GP from $10.6\% \pm 0.8\%$ to $33.6\% \pm 1.2\%$. Due to the additional

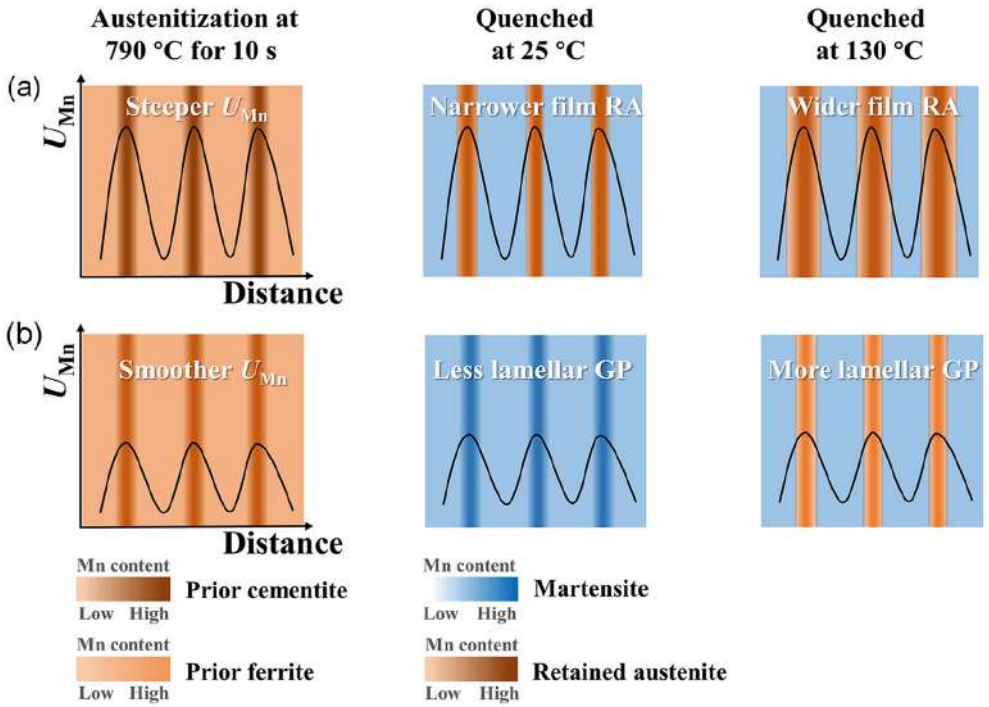

Fig. 4 Schematic illustration of effect of quenching temperature on width of film RA in lamellar GP (**a**) and fraction of lamellar GP (**b**)

carbon partitioning, many blocky RA islands are also present in QP sample, leading to a much larger RA fraction than that in DQ sample (25.7% versus 7.3%). The lamellar GP consists of alternative Mn-enriched RA and Mn-depleted lath martensite (Fig. 3c, d). Interestingly, the QP sample exhibits a larger width of film RA than the DQ sample (51.5 ± 4.4 nm versus 31.9 ± 5.9 nm), together with a lower U_{Mn} at martensite (M)/RA interface (4.0% versus 5.7%) (Fig. 3e). Similar phenomena are observed in Fe–0.42C–3.71Mn–1.45Si steel, as shown in Fig. 3f. After partitioned pearlite formation by holding at 590 °C for 6 h and the following austenitization, the fraction of lamellar GP is larger in QP samples than in the corresponding DQ samples. Additionally, after holding at 770 °C for 10 s, the QP sample has a larger width of film RA than the corresponding DQ sample (69.7 ± 7.6 nm versus 45.3 ± 6.0 nm) [20].

When the Mn-partitioned pearlite (Fig. 2b) is austenitized, the Mn distribution in high-temperature austenite is chemically patterned as illustrated in Fig. 4a. During quenching, the Mn-enriched austenite could be retained and the Mn depleted one could transform into martensite, leading to the GP formation (Fig. 3c, d). When increasing the quenching temperature, the driving force for austenite-to-martensite transformation is lowered. It is well-known that the Mn is austenite stabilizer as indicated by the relationship between Mn and martensite start transformation temperature (M_s) as listed in Eq. (1) [21, 22]:

$$M_s = 539 - 423w_C - 30.4w_{Mn} - 11w_{Si} \quad (1)$$

where w_C, w_{Mn} and w_{Si} represent the weight fraction of carbon, manganese and silicon, respectively. Thus, the austenite having a lower Mn content can be retained when the quenching temperature is higher (e.g., 130 °C in Fig. 4a). The U_{Mn} value at the interface between film RA and martensite is around 5.7% in DQ sample and 4.0% in QP sample (Fig. 3). During further partitioning at 400 °C, the carbon is enriched in austenite and the austenite stability is enhanced, leading to the retention of austenite after quenching to room temperature. Therefore, the width of film RA in QP samples is larger than that in corresponding DQ samples (Fig. 3f).

Increasing quenching temperature leads to an increased fraction of lamellar GP, which is also related to the reduction in driving force for martensite transformation. In the high-temperature austenite, some regions have a less intensity of chemical patterning, where the overall Mn content is lower and its distribution is smoother (Fig. 4b). When the quenching temperature is low (e.g., 25 °C), the austenite having less intensity of chemical patterning could fully transform to martensite; instead, when the quenching temperature is high (e.g., 130 °C), the austenite having less intensity of chemical patterning could still form GP

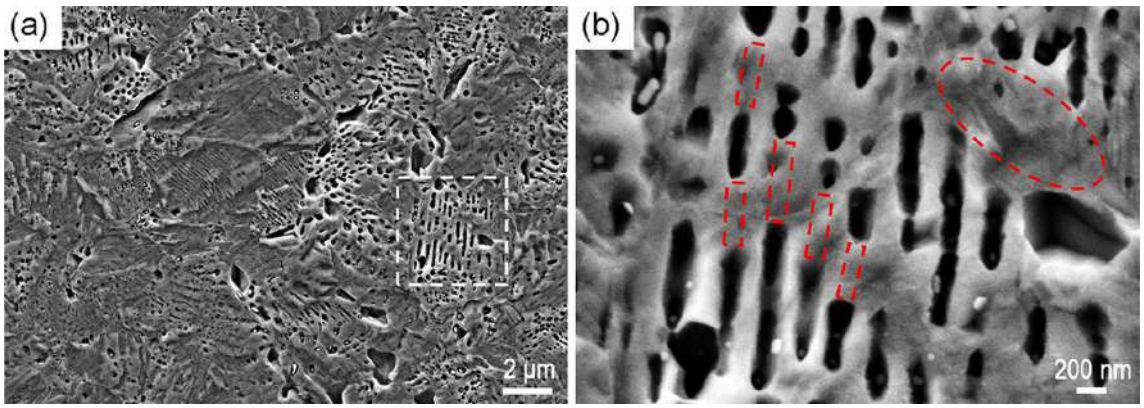

Fig. 5 SEM images of DQ sample (**a**) with an enlargement of white rectangle in **a** (**b**)

microstructure (Fig. 4b). As demonstrated in Fig. 5, although the lamellar GP is observed, several martensitic laths are connected with each other as indicated by red rectangles, and a circled region is fully martensite instead of alternative film RA and lath martensite probably due to the less intensity of Mn chemical patterning.

4 Conclusion

The lamellar ghost pearlite, which consists of alternative film RA and lath martensite, is formed in a chemical patterning way through fast austenitizing the partitioned pearlite. With increasing quenching temperature, the fraction of lamellar GP and the width of film RA in GP both increase. It is because a higher quenching temperature leads to a lower driving force for austenite-to-martensite transformation and, in turn, the retention of austenite having a lower Mn content. The current study provides a feasible way to enhance chemical patterning in medium-Mn steels through the adjustment of quenching temperature.

Acknowledgements Zhi-ping Xiong thanks the financial support from the National Natural Science Foundation of China (52271004 and 51901021) and the "Beijing Institute of Technology Research Fund Program for Young Scholars".

Declarations

Conflicts of interest There is no conflict of interest.

References

[1] K. Lu, Science 328 (2010) 319–320.
[2] B.C. De Cooman, Curr. Opin. Solid State Mater. Sci. 8 (2004) 285–303.
[3] F.G. Caballero, S. Allain, J. Cornide, J.D. Puerta Velásquez, C. Garcia-Mateo, M.K. Miller, Mater. Des. 49 (2013) 667–680.
[4] A. Perlade, A. Antoni, R. Besson, D. Caillard, M. Callahan, J. Emo, A.F. Gourgues, P. Maugis, A. Mestrallet, L. Thuinet, Q. Tonizzo, J.H. Schmitt, Mater. Sci. Technol. 35 (2019) 204–219.
[5] D. Frómeta, A. Lara, L. Grifé, T. Dieudonné, P. Dietsch, J. Rehrl, C. Suppan, D. Casellas, J. Calvo, Metall. Mater. Trans. A 52 (2021) 840–856.
[6] W.W. Sun, Y.X. Wu, S.C. Yang, C.R. Hutchinson, Scripta Mater. 146 (2018) 60–63.
[7] R. Ding, Y. Yao, B. Sun, G. Liu, J. He, T. Li, X. Wan, Z. Dai, D. Ponge, D. Raabe, C. Zhang, A. Godfrey, G. Miyamoto, T. Furuhara, Z. Yang, S. van der Zwaag, H. Chen, Sci. Adv. 6 (2020) 1430.
[8] J.H. Kim, G. Gu, M.H. Kwon, M. Koo, E.Y. Kim, J.K. Kim, J.S. Lee, D.W. Suh, Acta Mater. 223 (2022) 117506.
[9] S. Liu, B. Hu, W. Li, R.D.K. Misra, X. Jin, Scripta Mater. 194 (2021) 113636.
[10] S. Liu, Z. Xiong, H. Guo, C. Shang, R.D.K. Misra, Acta Mater. 124 (2017) 159–172.
[11] P. Wen, B. Hu, J. Han, H. Luo, J. Mater. Sci. Technol. 97 (2022) 54–68.
[12] M.S. Jeong, T.M. Park, S. Choi, S.J. Lee, J. Han, Scripta Mater. 190 (2021) 16–21.
[13] J.H. Kim, E.J. Seo, M.H. Kwon, S. Kang, B.C. De Cooman, Mater. Sci. Eng. A 729 (2018) 276–284.
[14] J.G. Speer, F.C.R. Assunção, D.K. Matlock, D.V. Edmonds, Mater. Res. 8 (2005) 417–423.
[15] Z.R. Hou, X.M. Zhao, W. Zhang, H.L. Liu, H.L. Yi, Mater. Sci. Technol. 34 (2018) 1168–1175.
[16] D.P. Koistinen, R.E. Marburger, Acta Metall. 7 (1959) 59–60.
[17] L. Liu, B.B. He, G.J. Cheng, H.W. Yen, M.X. Huang, Scripta Mater. 150 (2018) 1–6.
[18] Y.X. Wu, W.W. Sun, M.J. Styles, A. Arlazarov, C.R. Hutchinson, Acta Mater. 159 (2018) 209–224.
[19] D.Z. Yang, Z.P. Xiong, C. Zhang, G.Z. Feng, Z.F. Cheng, X.W. Cheng, J. Iron Steel Res. Int. 29 (2022) 1393–1403.
[20] C. Zhang, Z.P. Xiong, D.Z. Yang, X.W. Cheng, Acta Mater. 235 (2022) 118060.
[21] K.W. Andrews, J. Iron Steel Inst. 203 (1965) 721–727.
[22] J. Mahieu, B.C. De Cooman, J. Maki, Metall. Mater. Trans. A 33 (2002) 2573–2580.